King's Research Portal

Document Version
Peer reviewed version

[Link to publication record in King's Research Portal](#)

Calculating Kinetic Rates and Membrane Permeability from Biased Simulation

Magd Badaoui, Adam Kells, Carla Molteni, Callum J. Dickson, Viktor Hornak, and Edina Rosta

Just Accepted

1
2
3
4
5
6
7
8
9
10
11
12
13
14
15
16
17
18
19
20
21
22
23
24
25
26
27
28
29
30
31
32
33
34
35
36
37
38
39
40
41
42
43
44
45
46
47
48
49
50
51
52
53
54
55
56
57
58
59
60

Calculating Kinetic Rates and Membrane Permeability from Biased Simulations

Magd Badaoui[1], Adam Kells[1], Carla Molteni[2], Callum J. Dickson[3], Viktor Hornak[3] and Edina Rosta[1]*

[1]King's College London, Department of Chemistry, SE1 1DB, London, UK

[2]King's College London, Department of Physics, WC2R 2LS, London, UK

[3]Global Discovery Chemistry, Computer-Aided Drug Discovery, Novartis Institutes for BioMedical Re-search, 181 Mass Ave., Cambridge, MA 02139, USA

*Correspondence to: edina.rosta@kcl.ac.uk

ABSTRACT: We present a simple approach to calculate the kinetic properties of lipid membrane crossing processes from biased molecular dynamics simulations. We demonstrate that by using biased simulations, one can obtain highly accurate kinetic information with significantly reduced computational time with respect to unbiased simulations. We describe how to conveniently calculate the transition rates to enter, cross and exit the membrane in terms of mean first passage times. To obtain free energy barriers and relaxation times from biased simulations only, we constructed Markov models using the Dynamic Histogram Analysis Method (DHAM). The permeability coefficients that are calculated from the relaxation times are found to correlate highly with experimentally evaluated values. We show that more generally, certain calculated kinetic properties linked to the crossing of the membrane layer (e.g., barrier height and barrier crossing rates) are good indicators of ordering drugs by permeability. Extending the analysis to a 2D Markov model provides a physical description of the membrane crossing mechanism.
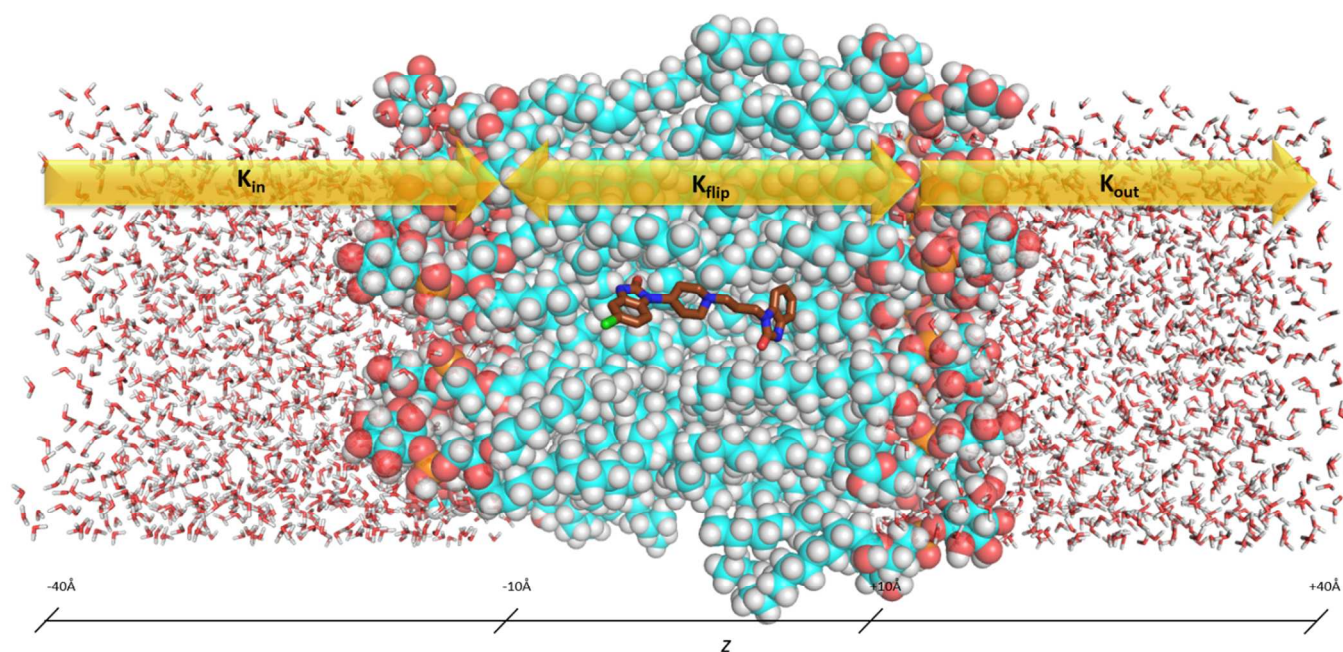
Figure 1. Representation of the system used in the molecular dynamics simulations: a drug molecule (in brown at center of image) interacts with and passes through a lipid membrane which is surrounded by water.

I. INTRODUCTION

For a drug to be effective, it has not only to bind strongly to its target, but it is also required to have good ADME (Absorption, Distribution, Metabolism, Excretion) profile[1]. An important factor for the absorption and the distribution is the drug's ability to cross the cell membrane to reach its target[2-4]. This has become particularly important for drugs that act in the central nervous system, and have to cross the blood brain barrier.[1] This property is traditionally estimated by the lipophilicity of the drug. However, taking into account only the lipophilicity of the molecule does not allow to fully understand the mechanism of membrane permeation (Fig. 1) and for this reason subsequent, more refined models take into account additional physical parameters, such as depth-dependent partitioning and the resistance coefficient of the membrane. For a fully quantitative description, it has become fundamental to predict the kinetic behaviour of drugs addressing membrane interaction and permeation.[1, 5-8] Studies related to the transport of small ligands crossing various phospholipid membranes are the subject of increased interest in recent years[5, 9-13]. There are also significant challenges to investigating this behaviour experimentally. Eyer et al.[14] proposed a liposomal fluorescence assay method by which the permeation of weak basic drug-like solutes across the lipid membrane can be determined. However, details of membrane crossing mechanisms at an atomistic level are still missing experimentally[14].
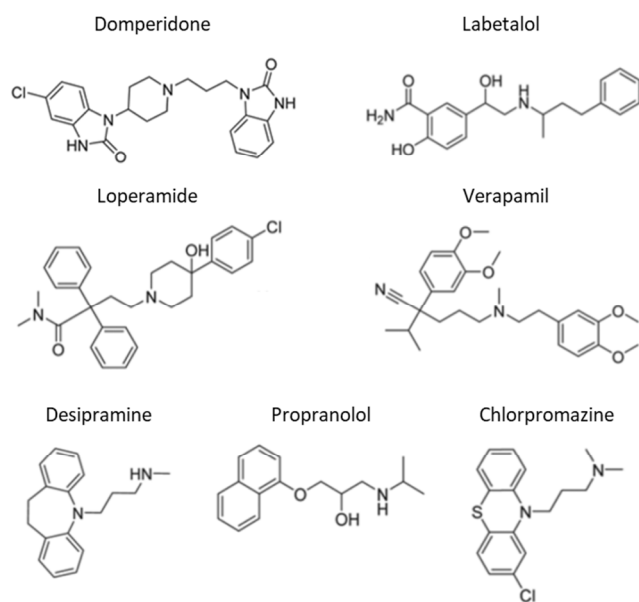

Figure 2. Chemical structure of the seven drugs analyzed by Eyer et al.[14]

Thanks to the dramatic recent development of computer technology , molecular dynamics (MD) simulations are now capable of reaching biologically significant timescales and are becoming widely used in the pharmaceutical industry[8, 15-25]. In tandem with the improvement in simulation hardware and software, an important role has been played by the construction of mathematical models which allow the vast volumes of MD data to be processed in a statistically optimal manner. Markov state models (MSMs) have emerged as a useful tool for analyzing and understanding the results of these simulations. In fact,

MSMs allow for the convenient combination of multiple MD trajectories into a single kinetic network model from which experimental observables and kinetic rates can be computed.[6, 13, 26-28]

Using experimentally obtained permeabilities by Eyer et al.[14] across a lipid membrane for seven structurally unrelated drugs (Fig. 2), Dickson et al.[29] recently demonstrated that accurate results for the permeability rates can be obtained by running long unbiased MD simulations[29]. By using an MSM formalism, kinetic rates of the key steps in membrane crossing can then be estimated. However, very large computational resources are required for a sufficiently converged set of unbiased simulation trajectories to be analyzed by MSMs. With the use of enhanced sampling biasing procedures, such as umbrella sampling (US), this computational time can be significantly reduced.

The construction of MSMs from biased simulation data has not been traditionally possible. Biased simulations require the potential energy function of the system of interest to be modified such that the system is for example harmonically restrained to a given region of the energy landscape. This is advantageous as it allows sampling of regions which might otherwise not be adequately visited during the simulation time. However, the kinetic behaviour observed is no longer representative of the true system and as such this needs to be accounted for when constructing the MSM. A recently derived unbiasing method, the Dynamic Histogram Analysis Method,(DHAM), by Rosta and Hummer[30] uses a maximum likelihood estimate of the MSM transition probabilities given the observed transition counts during each biased trajectory and is found to often produce more accurate results than those of the more commonly used weighted histogram analysis method (WHAM)[31]. This unbiasing method is the first to use only biased US simulation data to obtain kinetic information directly by constructing the unbiased MSM.

Here we determined the free energy profiles and kinetic rates of crossing a lipid membrane for the seven drugs in Fig. 2 by using US biased simulations. All experimental kinetic permeation data used for comparison for these seven drug molecules was previously obtained by Eyer et al[14]. Using this kinetic information, we aim to order the drugs according to their permeability coefficients (log Perm values). We analyzed US simulation data to calculate kinetic rates for the entry into the membrane, flipping, and exit from the membrane, and compared it with that obtained from long unbiased simulations. All MD simulation data (unbiased and US biased) was previously obtained by Dickson et al[29]. Here, we re-analyzed the US biased data to obtain molecular kinetic rates for the membrane permeation using DHAM[30]. We found an excellent agreement between the kinetic properties of the drugs from US biased simulations compared with those from the combined biased and unbiased MD simulations, which are also in agreement with experimental permeation measurements, demonstrating that these calculations provide accurate in silico kinetic rates for these important dynamical processes. Additionally, we analyzed the free energy surfaces corresponding to the orientations of the seven drugs molecules while crossing the membrane by determining MSMs on a two dimensional

(2D) surface using DHAM, describing in detail the orientation for three of them. This provides key insights into the drug permeation pathways and offers guidance for the design of molecules with required kinetic permeation properties.

II. METHOD

a. Markov State Modelling

An MSM consists of a set of memoryless conditional probabilities between user-defined discrete states (in our implementation along a finely discretized chosen reaction coordinate z), such that the value of $P(j,t|i,0)$ is the probability that the system is in state j at time t given that it was in state i initially. These conditional probabilities are typically calculated by determining the transition count matrix C_{ji}, which contains the count numbers of the observed transitions from state i to j. The time parameter t is called the lagtime and must be chosen sufficiently large such that the Chapman-Kolmogorov test[32] is satisfied (i.e. that the relaxation timescales, τ of the system are insensitive to changes in the lagtime).

To produce an MSM from enhanced sampling simulations in practice, we use a reaction coordinate of interest that was also employed to bias the MD simulation data. In the context of membrane permeation, it is desired to compute the kinetic rates with which the drug undergoes three important processes (see Fig. 1): the rate at which it enters into (k_{in}), crosses (k_{flip}), and exits (k_{out}) from the membrane. The corresponding reaction coordinate is the distance between the center of mass (COM) of the ligand and the center of the lipid membrane (z-coordinate as shown in Fig. 1) was used. Unlike in typical MSM models consisting of only metastable states, here we discretized this coordinate into bins, where the number of bins is chosen sufficiently large to give a finely discretized coordinate but not so large as to give an under-sampling of transitions between bins.

Once the bins have been determined, we count the number of observed transitions ($C_{ji}^{k}(t)$) between each pair of bins i and j in simulation k at the chosen lagtime t, as well as the number of times each bin is occupied ($n_i^k = \sum_j C_{ji}^k(t)$) during each simulation k. These values then provide the necessary conditional probabilities $M_{ji}(t) = P(j,t|i,0)$. In the simplest unbiased case not enforcing detailed balance strictly, the maximum likelihood estimates are given by:

$$M_{ji}(t) = \frac{\sum_k C_{ji}^k(t)}{\sum_k n_i^k} \qquad (1)$$

For biased simulations where a biasing energy of u_i^k is applied to state i during simulation k, we employed the

DHAM[30] to compute the unbiased MSM from the biased data as given by:

$$M_{ji}(t) = \frac{\sum_k C_{ji}^k(t)}{\sum_k n_i^k \exp(-(u_j^k - u_i^k)/2k_bT)} \qquad (2)$$

Eq. (2) reduces to the unbiased equation when the biasing potentials are set to zero. Once an MSM has been constructed from simulation data, one is typically interested in determining the free energy profile as well as the kinetic information (relaxation times and mean first passage times). These quantities can be computed directly from the eigenvalues λ_n and eigenfunctions ψ_n of the transition matrix. All the eigenvalues of the transition matrix with detailed balance fall between 1 and 0 and can be arranged in decreasing order:

$$1 = \lambda_1 > \lambda_2 \geq ... \geq \lambda_n > 0 \qquad (3)$$

The largest eigenvalue (equal to 1) gives the equilibrium populations of the states of the system (useful to find the free energy) while the second largest eigenvalue can be used to determine the timescale of the slowest relaxation process in the system via:

$$\tau_2 = \frac{-t}{\ln(\lambda_2)} \qquad (4)$$

The kinetic rates are computed by coarse graining our discretized states and corresponding free energy profile into four regions: the outer water, outer membrane, inner membrane and inner water regions (Fig. 1), using the Robust Perron Cluster Analysis (PCCA+) method[33] following Dickson et al.[29] Once the clusters have been specified, we calculate the rates (k_{in}, k_{flip} and k_{out}) from the Markov matrix as the inverse of the mean first passage times (MFPT)[34] between the regions.

The log Perm permeability values are typically calculated using Eq. (5):

$$\text{Perm} = \frac{k_{slow}r}{3} \qquad (5)$$

Where k_{slow} is defined to be the rate of the slowest process in the system, i.e. the process which is most significant in describing the decay of the populations to equilibrium and r is the radius of the liposome (100 nm). It should also be noted that in this context we use a base ten logarithm as is typically used when analyzing membrane permeability values. Typically, for membrane crossings, it is estimated by setting up a system of equations using the three rates (k_{in}, k_{flip} and k_{out}) as inputs, solving these equations in a kinetic network model and fitting the time dependent populations to a bi-exponential curve. Here we propose a simpler and more

direct approach to calculate the overall slowest relaxation time directly from the original Markov model and obtain a corresponding rate for k_{slow}. We compared and demonstrated that this simple approach is highly accurate and results in a similar k_{slow} estimate as the traditional approach.

Recently a number of advances of DHAM have been proposed where detailed balance is included[35-37]. We found that enforcing detailed balance did not lead to any observable changes in many US test cases we studied (data not shown), therefore here we used the simplest original DHAM approach via Eq. (2)[30, 35].

b.   Simulation Details

Compounds were modelled with the parm@Frosst force field, a small molecule force field that extends AMBER ff99SB,[38] and uses conformationally averaged AM1-BCC charges; lipids were modelled using the AMBER Lipid14 force field and water using TIP3P model. MD simulations were run with AMBER16 and PMEMD CUDA on GPU cards[39].

The starting structures for the US simulations are obtained by placing each ligand at the center of a POPC bilayer surrounded by water molecules (72 POPC and 60 waters per lipid)[40]. Three-dimensional periodic boundary conditions with the usual minimum image convention were employed. Energy minimization is performed by using the steepest descent method for 5000 steps and using the conjugate gradient method for further 5000 steps.

The system was then heated from 0 K to 100 K using Langevin dynamics within a 5 ps constant volume run, with restraints on the drug molecule and lipids using a force constant of 10 kcal mol^{-1} Å^{-2}. Subsequently, the volume was allowed to change freely increasing the temperature to 303 K. The Langevin collision frequency was ɣ=1 ps^{-1}; and anisotropic Berendsen control of the pressure around 1 atm was applied by coupling the periodic box with a time constant of 2 ps for 100 ps.

The equilibration was completed after an additional 5 ns with the pressure relaxation time reduced to 1 ps in NPT, removing the restrain on lipids. The SHAKE algorithm[41] was used to constrain the bonds involving hydrogen and a time step of 2 fs was used.

Using a pulling rate of 1 Å/ns the drugs were then pulled out from the center of the system to outside the membrane, for a total of 40 Å (force constant of 1.1 kcal mol^{-1} Å^{-2}), in the NPT ensemble with semi-isotropic pressure scaling. During the simulations, a snapshot was saved every 1 Å, from the center z=0 Å to z=40 Å generating 40 windows. The results were calculated for one bilayer leaflet and it was assumed that the second half behaves in the same way. This was achieved by reflecting the data along the z axis and adding 39 (Figs. S1-S8) or 40 windows (Fig. 5), depending on whether or not the window at z=0 Å was reflected as well. Each US window was run for 20 ns to allow equilibration followed by additional 80 ns of production run using an US force constant of 2.5 kcal mol^{-1} Å^{-2}. Configurations were recorded every 10 ps.

c.   2D-DHAM

Analogously to the 1D case, we constructed a finely discretized 2D grid to determine the MSMs along two reaction coordinates for the seven drugs.
Specifically for domperidone, loperamide and labetalol, we analyzed the rotational movement of the drug during its passage across the membrane.

As our first reaction coordinate we used the same z coordinate as previously (distance from ligand COM to membrane center). For our second coordinate, we use the projection of the molecular orientation vector onto the z co-
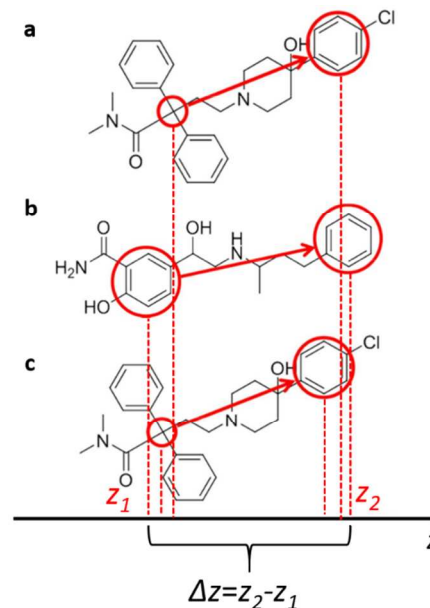
Figure 3. Definition of the Δz coordinate used in our 2D DHAM analysis. The values are obtained by projecting the vector along the drug molecules' length, as shown by the red arrows onto the z axis. The vector describing the molecular length joins the COM of the circled atoms as shown for Domperidone (**a**), Labetalol (**b**) and Loperamide (**c**).

ordinate Δz, as a measurement of the orientation of the ligand with respect to the membrane for two selected regions of the drug molecule along its length. Δz is equivalent to the molecular length scaled by the cosine of the angle between the z axes of the membrane and the molecular vector defined by the two ends of the ligand (Fig. 3). This means that when the ligand is oriented parallel to the membrane Δz will be around 0 Å as both ends are equidistant from the membrane, whereas when it is oriented perpendicular then Δz will be equal the end-to-end length of the ligand (around -10 to 10 Å). The extremities of the ligand can be the COM of distal functional groups (e.g. benzene) or single atoms, as shown in Fig. 3 for the molecules considered here.

This 2D-DHAM analysis and the 2D free energy surfaces are used to find correlations between the rotation of the ligand and its position across the membrane, showing

how the orientations of the ligand affect the free energies while crossing the membrane.

III. RESULTS AND DISCUSSION

a. MSM analysis of US simulations

Using the Markov modelling methods and US simulation trajectories, the relaxation time, τ_2, was calculated by constructing MSMs at a range of lagtimes up to 300 ps with 1000 bins as shown in Fig. 4. Using a recently derived method for calculating the limiting relaxation time of an MSM[42], we determined the long lagtime limit of the relaxation time for each drug as shown by the dashed lines in Fig. 4. The relaxation times can be seen to level off in the region of lagtimes greater than 100 ps. In the analysis that follows, we chose to use a lagtime of 200 ps, as it is sufficiently large for τ_2 to be insensitive to the precise choice of the lagtime. When calculating the MSMs with bin numbers of 600, 800, and 1000, at our chosen lagtime of 200 ps, there is almost no change in the obtained free energy profiles (Figs. S1-S7). We used 1000 bins for all subsequent analysis.
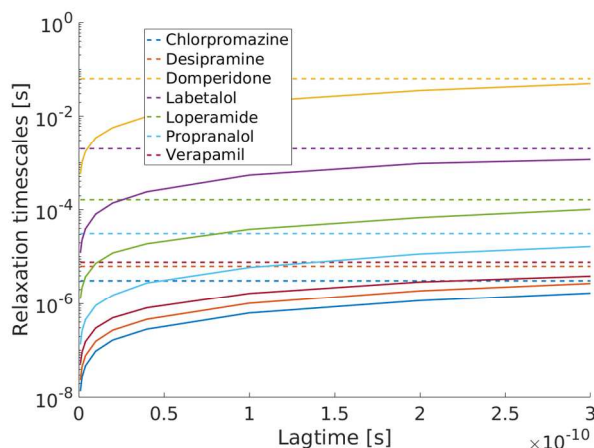

Figure 4. Relaxation time vs lagtime of the seven drugs (Fig. 2). The dashed lines represent the long lagtime limit of the relaxation time obtained by a least squares fitting to the relaxation times in the range of 1 ps to 300 ps.

Following this initial choice of parameters, seven Markov models were constructed with 1000 bins and a lagtime of 200 ps (100,000 simulation steps). This allows us to compute the free energy profiles for each drug and draw comparison with the profiles obtained in the unbiased simulations using WHAM (Fig. 5). Error bars were determined by dividing the data into two equal sections, determining the profiles independently and calculating the variance.

All our free energy profiles show the same trend as the one calculated by Dickson et al.[29] (dotted lines in Fig. 5) for the combined unbiased and biased MD data and indeed all the WHAM predictions fall within the margin of error for the DHAM results. While the PMF changes de-

pending on whether the US window at z=0 Å was reflected or not (Figs. 5 and S8), the log Perm data is essentially unchanged. The asymmetry observed in the not fully reflected PMF profiles also suggests that longer simulations might be needed to reduce the error at this transition region. At the same time, we used a fraction of the data required for the unbiased simulations. We obtained the kinetics profile using the US data by Dickson et al[29] with a total simulation time of 3.2 μs for each drug, whereas in the work done by Dickson et al.,[29] the calculation of the kinetic profile required multiple unbiased simulations, with a total simulation time of 12.5 μs per drug. By analyzing the US data with DHAM, we are able to reduce the total time by at least 75% over using unbiased data.

b. Ordering drugs according to their permeability

To determine the relative permeability, it is required to compare the rate of the slowest occurring process, k_{slow} corresponding to the crossing of the free energy barrier at the center of the membrane amongst the different drug molecules. Here we considered several ways to estimate the relative ordering (Table S1). Firstly, we can use the overall relaxation time corresponding to the second eigenvalue of the MSM constructed for each drug using Eq. (4). Secondly, we can make use of the free energy profile alone, and compare the height of the free energy barrier across the different drugs, using an Arrhenius relationship:

$$k_{slow} = Ae^{\frac{-\Delta G^{\ddagger}}{k_B T}} \quad (6)$$

Using the relaxation time obtained from the MSM in conjunction with the $\Delta G^{\ddagger}$ calculated from the populations, we can determine the Arrhenius prefactor. We obtained similar prefactors for all the drugs (Table S1), with an average value of 9.72 ± 5.76 e+07 s⁻¹, four orders of magnitude bigger than the typical value of $A = \frac{k_B T}{h}$ considering a transmission coefficient close to 1.

Thirdly, as the barrier corresponds to the flipping process, we can use the rate constants determined by mean first passage times, assuming $k_{slow} \approx k_{flip}$.

These three methods are each computationally simple to implement compared with alternative methods in the field of simulating a kinetic system from the calculated rates and performing a bi-exponential fit to the resultant time-dependent probabilities.

The biased and unbiased calculated log Perm values correlate very well with the experimental data (Fig. 6). The US simulation data displays similar R² values from the linear fit as the original kinetic data.

The log Perm values from the combination of unbiased and biased potential of mean force (PMF) data with the discrete transition based reweighting analysis method (dTRAM) of Dickson et al.[29] mostly lie above the experi-
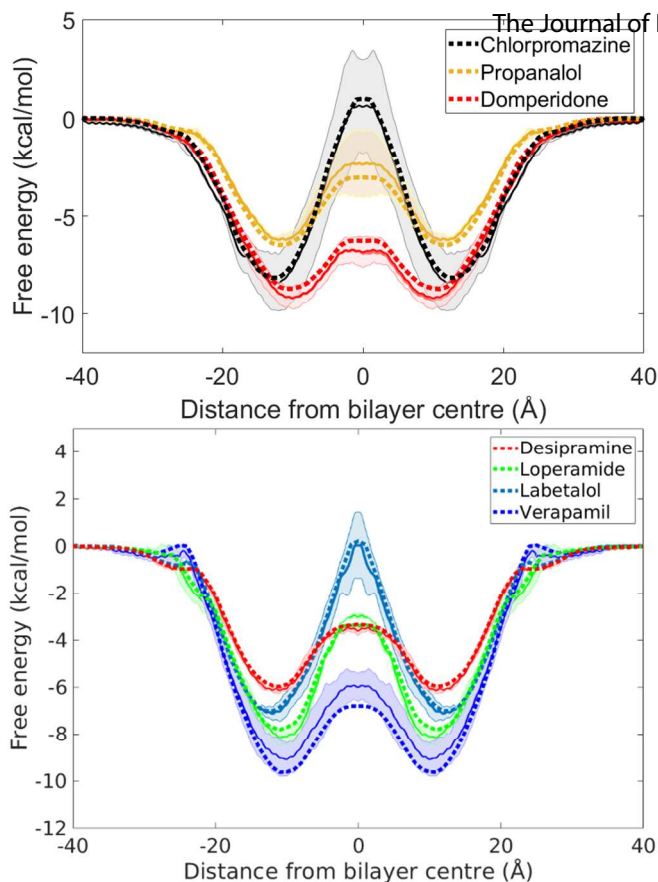
Figure 5. The free energy profiles calculated with DHAM from US simulations (solid lines) and WHAM using unbiased MD data (dashed lines). Errors are represented by shaded area for US data.

mental values predicting slightly faster permeation while the biased values are almost all below the line. This slow timescale might be because our model was calculated at a larger lagtime. Increasing the lagtime will increase the relaxation time and in turn decrease the value of the rate of the slowest process, resulting in a smaller permeability value. We expect that the most accurate simulation-based rate estimates are calculated from all data (biased and unbiased) using longer lagtimes.

Importantly, the process of ordering drugs according to their permeability is insensitive to the precise choice of lagtime. This can also be seen from Fig. 4, where the ordering of the lines does not change as a function of the lagtime, predicting the same ordering in a lagtime independent manner. This demonstrates that equivalently high correlations can be found between the experimental and biased data as with the unbiased data. Furthermore, using the simple approach of the relaxation time of the full Markov state model is an appropriate way to order the permeability of the drugs.
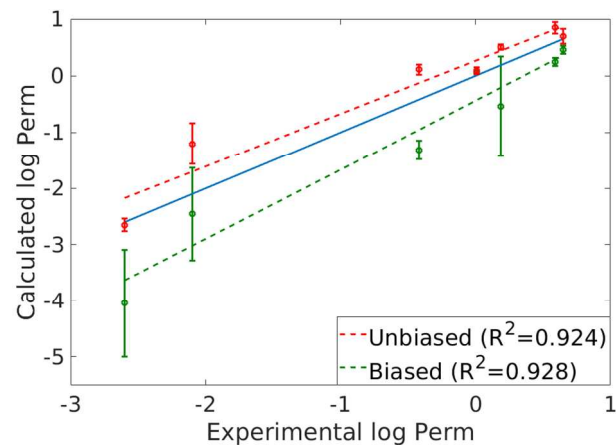

Figure 6. The log Perm values determined by the biased and unbiased simulations are compared with the experimental values[14, 29]. The correlation in between the data sets is comparably high for both the biased and unbiased simulations (both have p-values of well below the 5% required to be statistically significant).

By analyzing various kinetic quantities as predictors of the ordering of the drugs by permeability, we found that in general, any sensible choice of kinetic quantity which is closely related to the barrier crossing process will serve as an accurate indicator of drug ordering as shown in
Table S1.

The MSM relaxation times correlate very well with the calculated free energy barriers (Fig. S9). The corresponding permeation obtained from the free energy barrier heights using an Arrhenius rate expression with a constant prefactor of k_BT/h does not match the experimental log Perm values as closely as the MSM relaxation times, but because the R^2 calculations are invariant under linear transformations, the free energy barrier can also be used to calculate log Perm values accurately. However, if the permeation is investigated using different membrane compositions, the Arrhenius prefactor may vary, and a kinetic comparison using MSMs might become necessary.

c. 2D-DHAM

Using the 2D-DHAM analysis we calculated the 2D free energy surface of all seven drugs (Figs. S10-S16). Here we illustrate the results on three of them: domperidone, loperamide and labetalol, focusing on the rotation of the molecules while crossing the membrane.

We also verified that the free energy barriers from the 2D-DHAM analysis agree well with 1D-DHAM results.
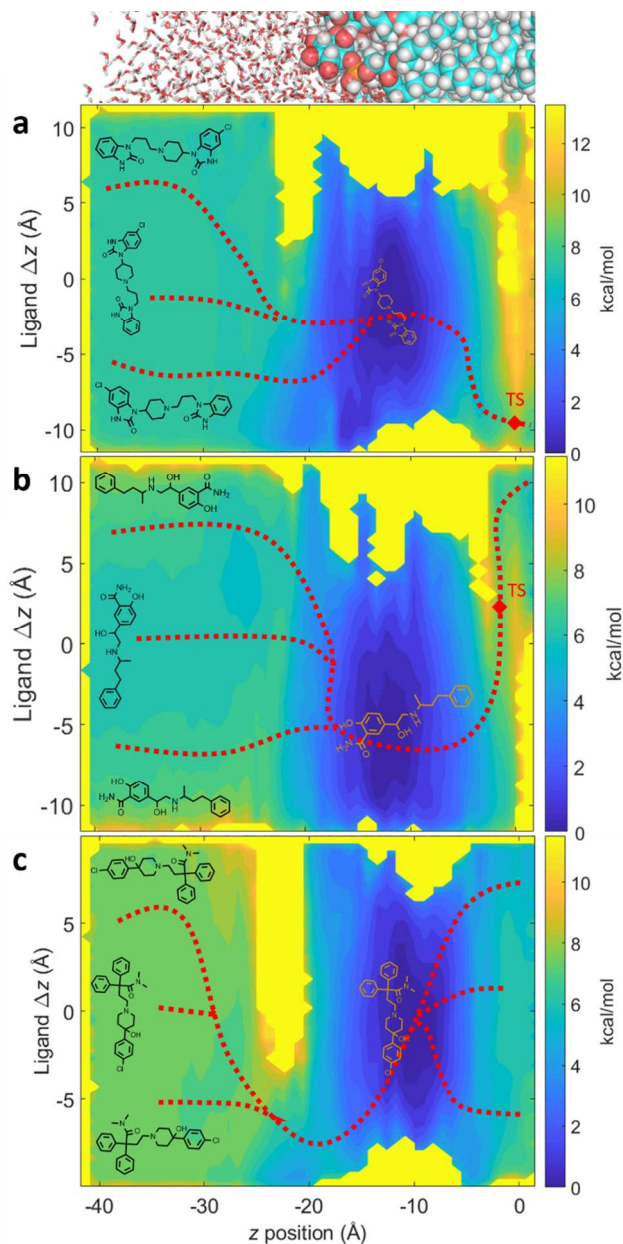
Figure 7: 2D free energy surfaces of (**a**) Domperidone, (**b**) Labetalol and (**c**) Loperamide along the absolute z position of the ligand, and the Δz coordinate for each molecule (schematic representation of the molecule orientation is also shown). The preferred paths for membrane crossing are shown as a function of the molecule orientation (red dotted lines).

Domperidone, Fig. 7(**a**), due to its polar characteristic, has a specific orientation inside the membrane. In the surrounding aqueous region the molecule is free to rotate its z position between -40 and -25 Å. Once near the membrane, domperidone has a preferential orientation parallel to the surface of the membrane. Between the inter lipid region and the polar head (0 Å < z < 20 Å) of the membrane it orientates perpendicular to the z coordinate showing a particular preference where the structure is parallel to the membrane surface.

Due to its dipole moment, in between the two-

phospholipidic layers, domperidone switches position preferring a parallel orientation with its more polar end pointing towards the water along z coordinate. This phenomenon is known as solute hopping[43].

The second compound, labetalol, Fig. 7(**b**) has an even stronger polar side, due to the presence of both hydroxyl groups and an amide group. On the other end, the molecule has a hydrophobic side, showing an overall "lipid-like" structure. When the drug is near the polar head of the membrane, it keeps its polar region close to the polar side of the membrane. Once at the intermembrane layer, it has a rapid interchange of orientation, keeping always its polar region close to the polar region of the membrane closest to bulk water.

Loperamide, Fig. 7(**c**), is the most hydrophobic of the three drugs, it prefers a specific orientation only when entering the membrane, with its hydroxylic group facing the membrane headgroups. Once entered, it tends to have relatively high rotational freedom.

As quantitatively assessed by 2D free energy surfaces as a function of the z and Δz coordinates, depending on the polarity and symmetry of the molecule, once inside the membrane, molecules have specific preferential orientations during the passage across the membrane. Several works have already been done to analyze the orientation of the ligands while crossing the membrane[44-47], and our results and general trends from the 2D-DHAM analysis agree with these previous works. Polar molecules keep their polar region facing towards the polar heads of the membrane, while more lipophilic compounds have a higher rotational freedom. Furthermore, polarity and charge distribution also determines the orientation of entry and the corresponding free energy pathways into the lipid membrane.

IV. CONCLUSION

We demonstrate that by performing a series of biased simulations of a drug molecule near a lipid membrane, highly accurate equilibrium and kinetic information can be determined by constructing an MSM using DHAM. This gives results which agree closely with experiment and achieve similar levels of accuracy as those attained by much longer unbiased MD simulations.

Furthermore, we present a simpler method for calculating permeability coefficients from MD simulation data by calculating the relaxation time directly from the MSMs. We also find that if the goal is to order the drugs according to permeability, then most kinetic quantities correlate with the free energy barrier to cross the membrane, indicating that linear transformations would give an excellent approximation to the experimental log Perm value. While this is very promising to order drugs in the same membrane environment, possibly such correlation with the barrier height no longer holds across different membrane/aqueous environments. We found that the prefactor in the Eyring equation differed by about four orders of magnitude from k_BT/h. This could potentially be due to the fact that the diffusion coefficients are very different

inside the membrane that has a very different dielectric constant than water, or could be due to other factors, including the choice of the reaction coordinates affecting the transmission coefficient.

Finally, we constructed 2D free energy surfaces and corresponding MSMs for three of our drug molecules and interpret the crossing mechanisms in terms of the physical processes occurring during the simulations. The molecular properties, *i.e.*, charge distribution and lipophilicity of the solute determine specific rotational preferences and pathways during the membrane entrance and crossing processes.

Our results demonstrate that DHAM is capable to provide accurate molecular kinetic information from purely biased simulations. As the range of systems with biased simulations is very flexible, we plan to apply this method in multiple applications. We can determine unbinding rates in molecular systems such as in host guest complexes, e.g., the competitive binding of ethanol and methanol with cucurbiturils in nano-aggregates of Au nanoparticles in aqueous environment[48], or for catalytic rates of enzyme catalyzed chemical reactions, such as e.g., the reaction mechanism of lipoxigenases[49]. Future work will be addressed to larger ligand permeability data sets, the kinetic prediction of ligand-protein unbinding and other important relevant kinetic processes.

Supporting Information

PMF profiles for the 7 studied drugs, permeability coefficient data, 2D free energy profiles.

REFERENCES

1.   Schuster, D.; Laggner, C.; Langer, T., Why Drugs Fail--a Study on Side Effects in New Chemical Entities. *Curr Pharm Des* **2005,** *11* (27), 3545-59.

2.   Smith, D.; Artursson, P.; Avdeef, A.; Di, L.; Ecker, G. F.; Faller, B.; Houston, J. B.; Kansy, M.; Kerns, E. H.; Krämer, S. D.; Lennernäs, H.; van de Waterbeemd, H.; Sugano, K.; Testa, B., Passive Lipoidal Diffusion and Carrier-Mediated Cell Uptake Are Both Important Mechanisms of Membrane Permeation in Drug Disposition. *Molecular Pharmaceutics* **2014,** *11* (6), 1727-1738.

3.   Avdeef, A., *Absorption and Drug Development: Solubility, Permeability, and Charge State*. John Wiley & Sons: 2012.

4.   Swift, R. V.; Amaro, R. E., Back to the Future: Can Physical Models of Passive Membrane Permeability Help Reduce Drug Candidate Attrition and Move Us Beyond Qspr? *Chem Biol Drug Des* **2013,** *81* (1), 61-71.

5.   Finkelstein, A., Water and Nonelectrolyte Permeability of Lipid Bilayer Membranes. *J Gen Physiol* **1976,** *68* (2), 127-35.

6.   Sezer, D.; Oruç, T., Protonation Kinetics Compromise Liposomal Fluorescence Assay of Membrane Permeation. *The Journal of Physical Chemistry B* **2017,** *121* (20), 5218-5227.

7.   Hermann, K. F.; Neuhaus, C. S.; Micallef, V.; Wagner, B.; Hatibovic, M.; Aschmann, H. E.; Paech, F.; Alvarez-Sanchez, R.; Krämer, S. D.; Belli, S., Kinetics of Lipid Bilayer Permeation of a Series of Ionisable Drugs and Their Correlation with Human Transporter-Independent Intestinal Permeability. *European Journal of Pharmaceutical Sciences* **2017,** *104*, 150-161.

8.   Amaro, R. E.; Mulholland, A. J., Multiscale Methods in Drug Design Bridge Chemical and Biological Complexity in the Search for Cures. *Nature Reviews Chemistry* **2018,** *2*, 0148.

9.   Krämer, S. D., Absorption Prediction from Physicochemical Parameters. *Pharmaceutical Science & Technology Today* **1999,** *2* (9), 373-380.

10.   Wessel, M. D.; Jurs, P. C.; Tolan, J. W.; Muskal, S. M., Prediction of Human Intestinal Absorption of Drug Compounds from Molecular Structure. *Journal of Chemical Information and Computer Sciences* **1998,** *38* (4), 726-735.

11.   Bemporad, D.; Essex, J. W.; Luttmann, C., Permeation of Small Molecules through a Lipid Bilayer: A Computer Simulation Study. *The Journal of Physical Chemistry B* **2004,** *108* (15), 4875-4884.

12.   Jagna, W.; Max, M.; G., K. B.; Markus, B.; Axel, M.; Trixie, W.; Sereina, R., Interconversion Rates between Conformational States as Rationale for the Membrane

Permeability of Cyclosporines. *ChemPhysChem* **2017,** *18* (23), 3309-3314.

13. Pokhrel, N.; Maibaum, L., Free Energy Calculations of Membrane Permeation: Challenges Due to Strong Headgroup–Solute Interactions. *Journal of chemical theory and computation* **2018,** *14* (3), 1762-1771.

14. Eyer, K.; Paech, F.; Schuler, F.; Kuhn, P.; Kissner, R.; Belli, S.; Dittrich, P. S.; Kramer, S. D., A Liposomal Fluorescence Assay to Study Permeation Kinetics of Drug-Like Weak Bases across the Lipid Bilayer. *J Control Release* **2014,** *173*, 102-9.

15. Marrink, S.-J.; Berendsen, H. J. C., Simulation of Water Transport through a Lipid Membrane. *The Journal of Physical Chemistry* **1994,** *98* (15), 4155-4168.

16. Xiang, T.-X.; Anderson, B. D., Liposomal Drug Transport: A Molecular Perspective from Molecular Dynamics Simulations in Lipid Bilayers. *Advanced Drug Delivery Reviews* **2006,** *58* (12), 1357-1378.

17. Ulander, J.; Haymet, A. D. J., Permeation across Hydrated Dppc Lipid Bilayers: Simulation of the Titrable Amphiphilic Drug Valproic Acid. *Biophysical Journal* **2003,** *85* (6), 3475-3484.

18. Tejwani, R. W.; Davis, M. E.; Anderson, B. D.; Stouch, T. R., Drug Discovery Interface: Functional Group Dependence of Solute Partitioning to Various Locations within a Dopc Bilayer: A Comparison of Molecular Dynamics Simulations with Experiment. *J. Pharm. Sci.* **2011,** *100* (6), 2136-2146.

19. Paloncyova, M.; Berka, K.; Otyepka, M., Convergence of Free Energy Profile of Coumarin in Lipid Bilayer. *Journal of Chemical Theory and Computation* **2012,** *8* (4), 1200-1211.

20. Carpenter, Timothy S.; Kirshner, Daniel A.; Lau, Edmond Y.; Wong, Sergio E.; Nilmeier, Jerome P.; Lightstone, Felice C., A Method to Predict Blood-Brain Barrier Permeability of Drug-Like Compounds Using Molecular Dynamics Simulations. *Biophysical Journal* **2014,** *107* (3), 630-641.

21. Tse, C. H.; Comer, J.; Wang, Y.; Chipot, C., Link between Membrane Composition and Permeability to Drugs. *Journal of chemical*

theory and computation **2018,** *14* (6), 2895-2909.

22. Zhu, Q.; Lu, Y.; He, X.; Liu, T.; Chen, H.; Wang, F.; Zheng, D.; Dong, H.; Ma, J., Entropy and Polarity Control the Partition and Transportation of Drug-Like Molecules in Biological Membrane. *Scientific Reports* **2017,** *7* (1), 17749.

23. Filipe, H. A. L.; Javanainen, M.; Salvador, A.; Galvão, A. M.; Vattulainen, I.; Loura, L. M. S.; Moreno, M. J., Quantitative Assessment of Methods Used to Obtain Rate Constants from Molecular Dynamics Simulations—Translocation of Cholesterol across Lipid Bilayers. *Journal of Chemical Theory and Computation* **2018,** *14* (7), 3840-3848.

24. Zhou, J.; Smith, M. D.; Cooper, S. J.; Cheng, X.; Smith, J. C.; Parks, J. M., Modeling of the Passive Permeation of Mercury and Methylmercury Complexes through a Bacterial Cytoplasmic Membrane. *Environmental Science & Technology* **2017,** *51* (18), 10595-10604.

25. Bemporad, D.; Luttmann, C.; Essex, J. W., Computer Simulation of Small Molecule Permeation across a Lipid Bilayer: Dependence on Bilayer Properties and Solute Volume, Size, and Cross-Sectional Area. *Biophys. J.* **2004,** *87* (1), 1-13.

26. Buchete, N. V.; Hummer, G., Coarse Master Equations for Peptide Folding Dynamics. *The Journal of Physical Chemistry. B* **2008,** *112* (19), 6057-69.

27. Pande, V. S.; Beauchamp, K.; Bowman, G. R., Everything You Wanted to Know About Markov State Models but Were Afraid to Ask. *Methods (San Diego, Calif.)* **2010,** *52* (1), 99-105.

28. Husic, B. E.; Pande, V. S., Markov State Models: From an Art to a Science. *J. Am. Chem. Soc.* **2018,** *140* (7), 2386-2396.

29. Dickson, C. J.; Hornak, V.; Pearlstein, R. A.; Duca, J. S., Structure-Kinetic Relationships of Passive Membrane Permeation from Multiscale Modeling. *J. Am. Chem. Soc.* **2017,** *139* (1), 442-452.

30. Rosta, E.; Hummer, G., Free Energies from Dynamic Weighted Histogram Analysis Using Unbiased Markov State Model. *Journal*

of Chemical Theory and Computation **2015,** *11* (1), 276-85.

31. Kumar, S.; Rosenberg, J. M.; Bouzida, D.; Swendsen, R. H.; Kollman, P. A., The Weighted Histogram Analysis Method for Free-Energy Calculations on Biomolecules. I. The Method. *Journal of Computational Chemistry* **1992,** *13* (8), 1011-1021.

32. Swope, W. C.; Pitera, J. W.; Suits, F., Describing Protein Folding Kinetics by Molecular Dynamics Simulations. 1. Theory. *The Journal of Physical Chemistry B* **2004,** *108* (21), 6571-6581.

33. Röblitz, S.; Weber, M., Fuzzy Spectral Clustering by Pcca+: Application to Markov State Models and Data Classification. *Advances in Data Analysis and Classification* **2013,** *7* (2), 147-179.

34. Meyer, C. D., An Alternative Expression for the Mean First Passage Matrix. *Linear Algebra and its Applications* **1978,** *22* (Supplement C), 41-47.

35. Stelzl, L. S.; Kells, A.; Rosta, E.; Hummer, G., Dynamic Histogram Analysis to Determine Free Energies and Rates from Biased Simulations. *Journal of Chemical Theory and Computation* **2017,** *13* (12), 6328-6342.

36. Stelzl, L. S.; Hummer, G., Kinetics from Replica Exchange Molecular Dynamics Simulations. *Journal of Chemical Theory and Computation* **2017,** *13* (8), 3927-3935.

37. Wu, H.; Paul, F.; Wehmeyer, C.; Noé, F., Multiensemble Markov Models of Molecular Thermodynamics and Kinetics. *Proceedings of the National Academy of Sciences* **2016,** *113* (23), E3221-E3230.

38. Hornak, V.; Abel, R.; Okur, A.; Strockbine, B.; Roitberg, A.; Simmerling, C., Comparison of Multiple Amber Force Fields and Development of Improved Protein Backbone Parameters. *Proteins* **2006,** *65* (3), 712-25.

39. D.A. Case, D. S. C., T.E. Cheatham, III, T.A. Darden, R.E. Duke, T.J. Giese, H. Gohlke, A.W. Goetz, D. Greene, N. Homeyer, S. Izadi, A. Kovalenko, T.S. Lee, S. LeGrand, P. Li, C. Lin, J. Liu, T. Luchko, R. Luo, D. Mermelstein, K.M. Merz, G. Monard, H. Nguyen, I. Omelyan, A. Onufriev, F. Pan, R. Qi, D.R. Roe, A. Roitberg, C. Sagui, C.L. Simmerling, W.M.

Botello-Smith, J. Swails, R.C. Walker, J. Wang, R.M. Wolf, X. Wu, L. Xiao, D.M. York and P.A. Kollman,, Amber 2017. **2017**.

40. Dickson, C. J.; Madej, B. D.; Skjevik, Å. A.; Betz, R. M.; Teigen, K.; Gould, I. R.; Walker, R. C., Lipid14: The Amber Lipid Force Field. *Journal of Chemical Theory and Computation* **2014,** *10* (2), 865-879.

41. Ryckaert, J.-P.; Ciccotti, G.; Berendsen, H. J. C., Numerical Integration of the Cartesian Equations of Motion of a System with Constraints: Molecular Dynamics of N-Alkanes. *Journal of Computational Physics* **1977,** *23* (3), 327-341.

42. Kells, A.; Annibale, A.; Rosta, E., Limiting Relaxation Times from Markov State Models. *The Journal of Chemical Physics* **2018,** *149* (7), 072324.

43. Trauble, H., The Movement of Molecules across Lipid Membranes: A Molecular Theory. *J. Membr. Biol.* **1971,** *4* (1), 193-208.

44. Bemporad, D.; Luttmann, C.; Essex, J. W., Behaviour of Small Solutes and Large Drugs in a Lipid Bilayer from Computer Simulations. *Biochimica et Biophysica Acta (BBA) - Biomembranes* **2005,** *1718* (1), 1-21.
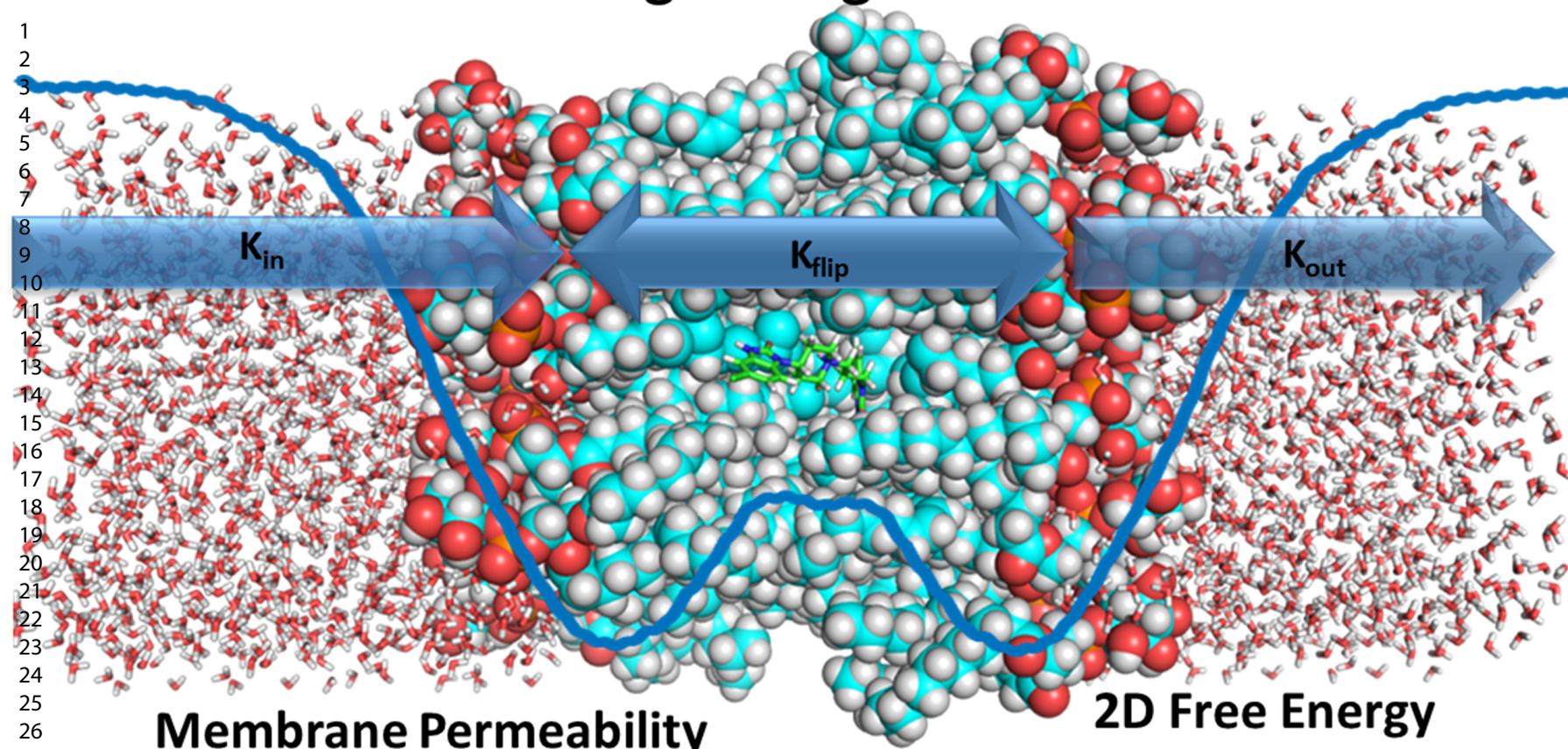
45. Orsi, M.; Noro, M. G.; Essex, J. W., Dual-Resolution Molecular Dynamics Simulation of Antimicrobials in Biomembranes. *Journal of the Royal Society, Interface* **2011,** *8* (59), 826-41.

46. Orsi, M.; Essex, J. W., Permeability of Drugs and Hormones through a Lipid Bilayer: Insights from Dual-Resolution Molecular Dynamics. *Soft Matter* **2010,** *6* (16), 3797-3808.

47. Sun, R.; Dama, J. F.; Tan, J. S.; Rose, J. P.; Voth, G. A., Transition-Tempered Metadynamics Is a Promising Tool for Studying the Permeation of Drug-Like Molecules through Membranes. *Journal of Chemical Theory and Computation* **2016,** *12* (10), 5157-5169.

48. de Nijs, B.; Kamp, M.; Szabo, I.; Barrow, S. J.; Benz, F.; Wu, G.; Carnegie, C.; Chikkaraddy, R.; Wang, W.; Deacon, W. M.; Rosta, E.; Baumberg, J. J.; Scherman, O. A., Smart Supramolecular Sensing with Cucurbit[N]Urils: Probing Hydrogen Bonding with Sers. *Faraday Discuss.* **2017,** *205*, 505-515.

49.   Suardíaz, R.; Jambrina, P. G.; Masgrau, L.; González-Lafont, À.; Rosta, E.; Lluch, J. M., Understanding the Mechanism of the Hydrogen Abstraction from Arachidonic Acid Catalyzed by the Human Enzyme 15-Lipoxygenase-2. A Quantum Mechanics/Molecular Mechanics Free Energy Simulation. *Journal of Chemical Theory and Computation* **2016,** *12* (4), 2079-2090.

1
2
3
4
5
6
7
8
9
10
11
12
13
14
15
16
17
18
19
20
21
22
23
24
25
26
27
28
29
30
31
32
33
34
35
36
37
38
39
40
41
42
43
44
45
46
47
48
49
50
51
52
53
54
55
56
57
58
59
60

Drug Passage Kinetics

K_{in}

K_{flip}

K_{out}

Membrane Permeability

2D Free Energy

Unbiased (R^2=0.924)

Biased (R^2=0.928)